Available online at www.sciencedirect.com
ScienceDirect
Ceramics International 34 (2008) 2001–2006
CERAMICS INTERNATIONAL
www.elsevier.com/locate/ceramint

Doped and Co-doped CeO_2: Preparation and properties

Snezana B. Bošković [a,*], Dejan R. Djurović [a], Slavica P. Zec [a], Branko Z. Matović [a], Matvei Zinkevich [b], Fritz Aldinger [b]

[a] *Institute of Nuclear Sciences Vinča, 11001 Belgrade, Serbia*
[b] *Max-Planck Institute, PML, Stuttgart, Germany*

Received 4 May 2007; received in revised form 29 June 2007; accepted 21 July 2007
Available online 30 August 2007

Abstract

Glycine/nitrate method was modified and applied to synthesize ceria solid solutions doped with rare earth cations and yttrium (Gd, Sm, Nd, Y) in the concentration range $0 \leq x \leq 0.25$. The modification of glycine nitrate process was performed by substituting a portion of Ce-nitrate with the less expensive Ce-acetate. Nanometric size powder particles were obtained. Powder properties such as specific surface area, crystallite and particle size, dopants content and lattice parameters have been studied. The results showed that the dopants used in the mentioned concentration range formed solid solutions with host ceria. Defect model introducing anion vacancy radius can be applied to calculate lattice parameters and theoretical densities of doped and four-fold co-doped ceria nanosized solid solutions.

Keywords: Nanosized CeO_2; Solid solutions; Chemical synthesis; Properties

1. Introduction

Ceria as well as ceria based materials are attractive for many applications like components for SOFC, various catalysts, oxygen sensors, polishing materials, etc. Recently, nanometric size ceria attracted much attention because the application of the nanometric particles improves some properties such as electrical conductivity and catalytic behavior while also decreasing sintering temperature. In that way the cost of final products is reduced through the lower energy consumption.

The success of many promising technologies is entirely dependent on the development of powders synthesis techniques [1]. Great variety of methods for nanosized powder synthesis has been published in the literature [2–5]. The challenge for these new synthesis techniques is to preserve high powder activity while attaining the desired complex composition. Produced powders must be clean, nanosized, with precise stoichiometry and homogeneously distributed dopant cations throughout the batch. The method applied should give reproducible powder properties, high yield and must be time and energy effective.

Glycine nitrate process [6,7] is based in the exothermicity of the redox reaction between the fuel–glycine and oxidizer-nitrate. The procedure needs to be performed in three stages, which are as follows: dissolution of metal nitrates and glycine in water, autoignition of solution at about 180 °C, that afterwards undergoes the selfsustaining combustion giving ash as a product, and finally calcination of ash to burn out organic components producing a clean homogeneous oxide powder of the required stoichiometry. When the addition of dopants is desirable many of them may be simultaneously incorporated into the host lattice [8].

The electrical conductivity of SOFC electrolyte is affected by ionic radii of dopants [9]. The conductivity is higher if the mismatch in ionic sizes of host and dopant cations is as low as possible [10]. On the other hand, it was shown that the activation energy of O^{2-} migration for co-doped samples with five or ten different dopants was lower, whereas the electrical conductivity was by 30% higher, as compared to best single doped samples with the same vacancy concentration [9].

In this paper the results on the synthesis and properties of fluorite type pure ceria powder, doped ceria powders with Re cations in the concentration range $0 \leq x \leq 0.25$, as well as co-doped powder are described. To our knowledge the modified glycine/nitrate procedure (MGNP) [8] was used for the first time to synthesize ceria powders.

* Corresponding author.

0272-8842/$34.00
doi:10.1016/j.ceramint.2007.07.036

2. Experimental

2.1. Synthesis

Starting chemicals used for the synthesis of powders were glycine, cerium acetate hydrate, cerium nitrate hexahydrate and Re nitrates hexahydrates (Gd, Sm, Nd, Y from Alfa Aesar GmbH, Germany). Reacting solution consisted of Ce-acetate, Ce-nitrate, Re-nitrate and glycine, in the ratio depending on the final composition, with approximately a 100 ml of distilled water. Glycine to nitrate ratio in the solution was kept constant—1:1. All nitrate solutions were previously prepared and the cation concentration (in mg/ml) was determined by titration with EDTA. On the basis of these data, the portion of each premix was added according to a previously calculated composition of the final powder. The acetate and glycine were added in the powdered form by weighing required portions. A stainless steel beaker was used as a reactor. The solutions were heated in the air using a muffle furnace. The burn-up process was terminated at about 450 °C and the ash powders were obtained. As a result of modifying GNP, the reactions proceeded very smoothly. Therefore, almost no loss in the synthesized powders quantity was observed. The experimentally obtained amount of powders was in the range from 96 to 99%, i.e. very close to the theoretical calculations. For practical reasons it is very important to point out that the quantity of chemicals in the mixture was designed to synthesize 100 g of powder per run (in 30 min), which, presumably, is the largest scale produced by this method so far. Since the evaporation was not intense during the experiment, the amount of powder produced per run can be even higher using a reactor with larger dimensions. The obtained ashes were later calcined at 600 °C for 4 h. Beside doped ceria, co-doped powder was also synthesized. This powder will be used in future work with the idea to enhance the electrical conductivity of doped samples compared to single doped material.

2.2. Characterization

X-ray diffraction analysis (XRD) was used to identify the crystalline phases as well as the lattice parameters of solid solution powders. The diffracted X-rays were collected over 2θ range 20–80° using a step width of 0.02° and measuring for 1 s per step. Before measurement the diffractometer was calibrated using high quality Si standard. Lattice parameters of all synthesized powders were calculated from diffraction lines using Win Cell software based on the least square procedure. The standard deviation was about 1%. Williamson-Hall plots were used to separate the effect of the size and strain in the nanocrystals [9].

The specific surface area was determined using modified BET method. In addition, SEM (Zeiss) was performed to characterize the morphology and particle size of the calcined powders.

Classical chemical analysis was performed to determine the difference between nominal and final composition of the synthesized powders.

3. Results and discussion

Glycine plays a double role during the reaction: it serves as a fuel and as a complexant. Glycine complexes the metal cations thus preventing their selective precipitation as water is evaporated during the procedure. The process can be modified by varying the glycine to nitrate ratio, as it is conventionally performed. However, we modified this process by substituting part of nitrates for acetates in the same cation. Acetates are also soluble in water and, in addition, are less expensive. Thus, the reaction temperature is decreased affecting both the intensity of burn up stage and the particle size. It should be also emphasized that the process is flexible for producing complex compositions as shown previously [8], for perovskite structures whereby both A and B lattice sites were substituted simultaneously.

The glycine/nitrate process is based on the reaction between glycine and nitrates according to the reaction:

$$4C_2H_5NO_2 + 2\{(1-x)Ce(NO_3)_3{\cdot}6H_2O\} + 2\{xMe(NO_3)_3{\cdot}6H_2O\} + 2O_2 \rightarrow 2Ce_{1-x}Me_xO_{2-y} + 22H_2O\uparrow + 5N_2\uparrow + 8CO_2\uparrow \quad (1)$$

that gives doped ceria solid solution powders as a reaction product. The reaction after ignition, proceeds spontaneously and terminates extremely fast with the strong release of gaseous products as in accordance with the above reaction. It takes about 30 min to produce one batch of powder. In our case the glycine to nitrate ratio was 1:1, and was kept constant throughout the experimental work. Half of the calculated fraction of Ce ions originated from nitrates and the other half from acetates, while all the dopant cations were obtained from nitrates.

After ignition the ashes were usually single phase as shown by the XRD, as illustrated for yttria doped ceria in Fig. 1. Diffraction lines were diffuse, indicating smaller crystallite size. However, all the ashes were calcined to ensure the burn out the organic reaction products. XRD pattern of calcined powder is also shown in Fig. 1. The results in Fig. 2 shows XRD diffraction pattern of calcined codoped sample. Figs. 1 and 2

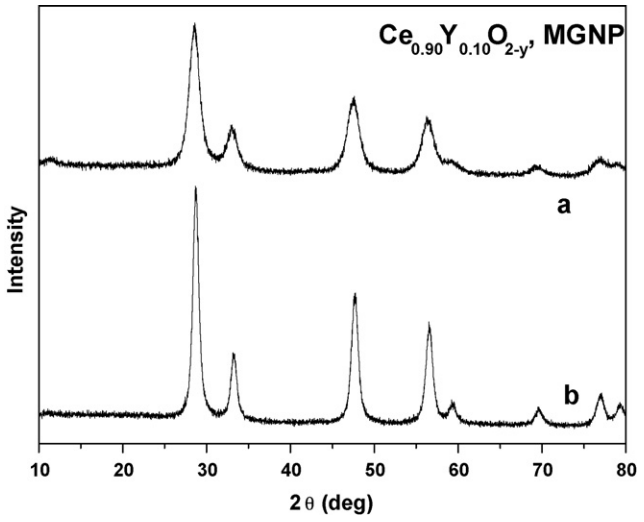

Fig. 1. XRD pattern of Y doped ceria: (a) ash, (b) calcined at 600 °C, 4 h.

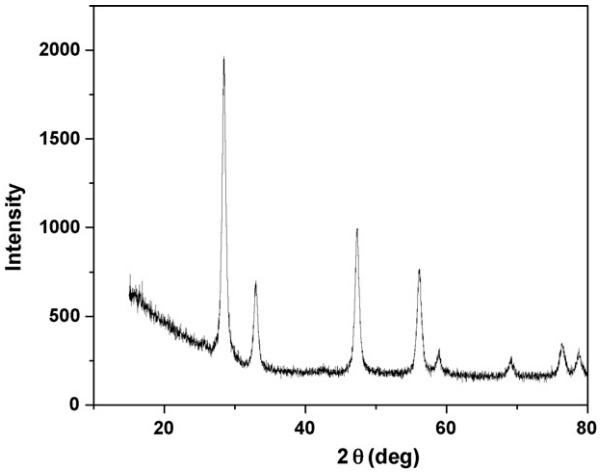

Fig. 2. XRD pattern of calcined $Ce_{0.80}Y_{0.05}Gd_{0.05}Nd_{0.05}Sm_{0.05}O_{2-y}$.

show that both doped and co-coped samples were single phase compositions before and after calcination.

Dopants concentrations in the final solid solutions determined by EDTA titration are given in Table 1. Significant match between nominal and final compositions is obvious. For co-doped sample total the value of x is 0.206 compared to nominal 0.20, and the composition may be expressed as a stoichiometric formula $Ce_{0.794}Y_{0.068}Nd_{0.052}Sm_{0.046}Gd_{0.040}O_{2-y}$.

Although the diffraction lines of the calcined samples (Fig. 1b) are much sharper and stronger, the powders obtained were nanometric in size (all powders are in the range between 18 and 30 nm, as determined by SEM measurements), which is illustrated for yttria doped ceria in Fig. 3.

Calculated on the basis of XRD data the crystallite size for all of the powders is less than 20 nm (Table 2), which, when compared with SEM data, indicates that the powders were not strongly agglomerated. Crystallite size shows an increasing trend with increasing dopant concentration.

Although generally very small microstrain values show that the lattice of the prepared powders is slightly constraint. However there is no evidence of any regularity caused by increasing dopants radii or concentrations. It is interesting to note that the co-doped sample retains very small value of microstrain.

Table 1
Chemical analysis of dopants content and the final x value in $Ce_{1-x}Re_xO_{2-y}$

Nominal composition	Dopants content (wt.%)	x in $Ce_{1-x}Re_xO_{2-y}$
$Ce_{0.9}Y_{0.1}O_{2-y}$	9.63 ± 0.10	0,107
$Ce_{0.75}Y_{0.25}O_{2-y}$	13.68 ± 0.14	0.248
$Ce_{0.9}Gd_{0.1}O_{2-y}$	9.93 ± 0.10	0.108
$Ce_{0.75}Gd_{0.25}O_{2-y}$	23.4 ± 0.20	0.260
$Ce_{0.9}Sm_{0.1}O_{2-y}$	9.15 ± 0.10	0.105
$Ce_{0.75}Sm_{0.25}O_{2-y}$	21.1 ± 0.20	0.247
$Ce_{0.9}Nd_{0.1}O_{2-y}$	8.57 ± 0.08	0.101
$Ce_{0.75}Nd_{0.25}O_{2-y}$	19.52 ± 0.20	0.240
$Ce_{0.8}Y_{0.05}Nd_{0.05}Sm_{0.05}Gd_{0.05}O_{2-y}$		
Nd	4.44 ± 0.04	0.052
Sm	6.37 ± 0.06	0.046
Gd	6.40 ± 0.06	0.040
Y	3.60 ± 0.04	0.068

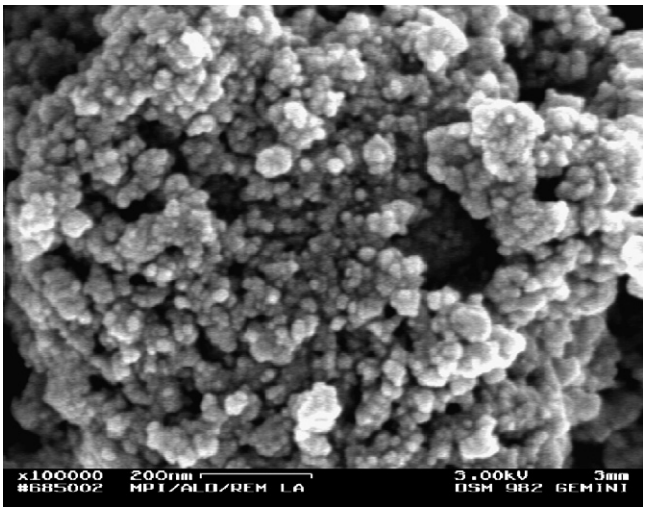

Fig. 3. SEM of MGNP prepared $Ce_{0.9}Y_{0.1}O_{2-x}$ powder calcined at 600 °C, 4 h.

Specific surface area change versus dopants concentration is given in Table 3. In some cases, the linearity of the dependence of specific surface area on dopants content holds quite satisfactory, e.g., with increasing Y concentration specific surface area tends to increase. With the rare earth dopants, however, specific surface area tends to decrease with increasing dopants concentration.

Co-doped sample retained the rather high value of specific surface area of 40.68 m^2/g which is in agreement with small crystallite size of the sample.

Lattice parameters of all studied solid solutions (Fig. 4), show a linear dependence on the doping level in the investigated composition range. In the case of Y^{3+} as a dopant, the lattice parameter decreases with increasing Y concentration, which was also found in earlier work [11]. The reason for this behavior may be that with increasing Y content, oxygen vacancy concentration increases, although the ionic radius of

Table 2
XRD characteristics of solid solutions

Sample no.	Composition	Crystallite size (nm)	Mean microstrains $\varepsilon \times 10^4$
1	CeO_2	17(±2)	1.3
2	$Ce_{0.9}Y_{0.1}O_{2-y}$	10(±1)	0.3
3	$Ce_{0.85}Y_{0.15}O_{2-y}$	15(±1)	1.7
4	$Ce_{0.8}Y_{0.2}O_{2-y}$	17(±2)	9.3
5	$Ce_{0.75}Y_{0.25}O_{2-y}$	16(±2)	2.7
6	$Ce_{0.9}Gd_{0.1}O_{2-y}$	16(±2)	3.5
7	$Ce_{0.85}Gd_{0.15}O_{2-y}$	18(±2)	0.4
8	$Ce_{0.8}Gd_{0.2}O_{2-y}$	15(±1)	2.6
9	$Ce_{0.75}Gd_{0.25}O_{2-y}$	20(±2)	2.8
10	$Ce_{0.9}Sm_{0.1}O_{2-y}$	14(±1)	4.5
11	$Ce_{0.85}Sm_{0.15}O_{2-y}$	15(±1)	6.5
12	$Ce_{0.8}Sm_{0.2}O_{2-y}$	17(±2)	3.2
13	$Ce_{0.75}Sm_{0.25}O_{2-y}$	19(±2)	3.3
14	$Ce_{0.9}Nd_{0.1}O_{2-y}$	14(±1)	2.2
15	$Ce_{0.85}Nd_{0.15}O_{2-y}$	16(±2)	4.4
16	$Ce_{0.8}Nd_{0.2}O_{2-y}$	15(±1)	2.6
17	$Ce_{0.75}Nd_{0.25}O_{2-y}$	15(±1)	1.2
18	$Ce_{0.8}Y_{0.05}Nd_{0.05}Sm_{0.05}Gd_{0.05}O_{2-y}$	13(±1)	2.1

Table 3
Specific surface area of nanostructured doped ceria solid solutions calcined at 600 °C, 4 h

Composition	Specific surface area (m^2/g)
CeO_2	34.85
$Ce_{0.90}Y_{0.10}O_{2-y}$	37.69
$Ce_{0.85}Y_{0.15}O_{2-y}$	36.76
$Ce_{0.80}Y_{0.20}O_{2-y}$	40.21
$Ce_{0.75}Y_{0.25}O_{2-y}$	40.64
$Ce_{0.90}Gd_{0.10}O_{2-y}$	40.10
$Ce_{0.85}Gd_{0.15}O_{2-y}$	33.55
$Ce_{0.80}Gd_{0.20}O_{2-y}$	35.94
$Ce_{0.75}Gd_{0.25}O_{2-y}$	29.71
$Ce_{0.90}Sm_{0.10}O_{2-y}$	43.16
$Ce_{0.85}Sm_{0.15}O_{2-y}$	40.98
$Ce_{0.80}Sm_{0.20}O_{2-y}$	35.48
$Ce_{0.75}Sm_{0.25}O_{2-y}$	31.79
$Ce_{0.90}Nd_{0.10}O_{2-y}$	43.33
$Ce_{0.85}Nd_{0.15}O_{2-y}$	40.86
$Ce_{0.80}Nd_{0.20}O_{2-y}$	35.60
$Ce_{0.75}Nd_{0.25}O_{2-y}$	41.37
$Ce_{0.80}Y_{0.05}Nd_{0.05}Gd_{0.05}Sm_{0.05}O_{2-y}$	40.68

Y^{3+} is slightly larger than that of Ce^{4+}(1.019 and 0.97 Å, respectively).

In other cases (Gd^{3+}, Sm^{3+}, Nd^{3+}), the lattice parameters increase with increasing fraction of dopant cations in the lattice. In addition, the results in Fig. 4 show an expected increasing slope of straight lines with increasing Re^{3+} radius. The lattice parameter of pure nanometric ceria was 5.407 Å similar to that obtained by Zhang et al. [13], whereas the value of $Ce_{0.794}Y_{0.068}Nd_{0.052}Sm_{0.046}Gd_{0.040}O_{2-y}$ lattice parameter is 5.434 Å.

In our previous publications [14,15] the existence of extrinsic and intrinsic vacancies in finer (4–6 nm) nanosized particles of ceria solid solutions was proved by Raman spectroscopy. That is why we applied the model introducing effective anion vacancy radius [12] for the lattice parameter calculation. This model was developed for single doped solid solutions. Lattice parameters were calculated according to equation:

$$a = \frac{4}{\sqrt{3}}[x{r_M}^{3+} + (1-x){r_{Ce}}^{4+} + (1-0.25x){r_O}^{2-} + 0.25x r_{Vo}]0.9971 \quad (2)$$

using the ionic radii from the Shannon's compilation [16] and experimentally obtained values of x from Table 1.

From the results also given in Fig. 4, it is obvious that very good agreement exists between measured and calculated lattice parameters for single doped solid solutions was obtained, again with the exception of Y doped ceria. Further clarification is needed to find out if the defect clusters that form in Y doped ceria [17] are responsible for the difference in measured and calculated lattice parameters.

To calculate lattice parameter of co-doped solid solution, we applied the same model, whereby average ionic radius was introduced instead of individual radii of all of dopants present in the lattice. The average ionic radius was obtained from experimentally measured lattice parameters with constant

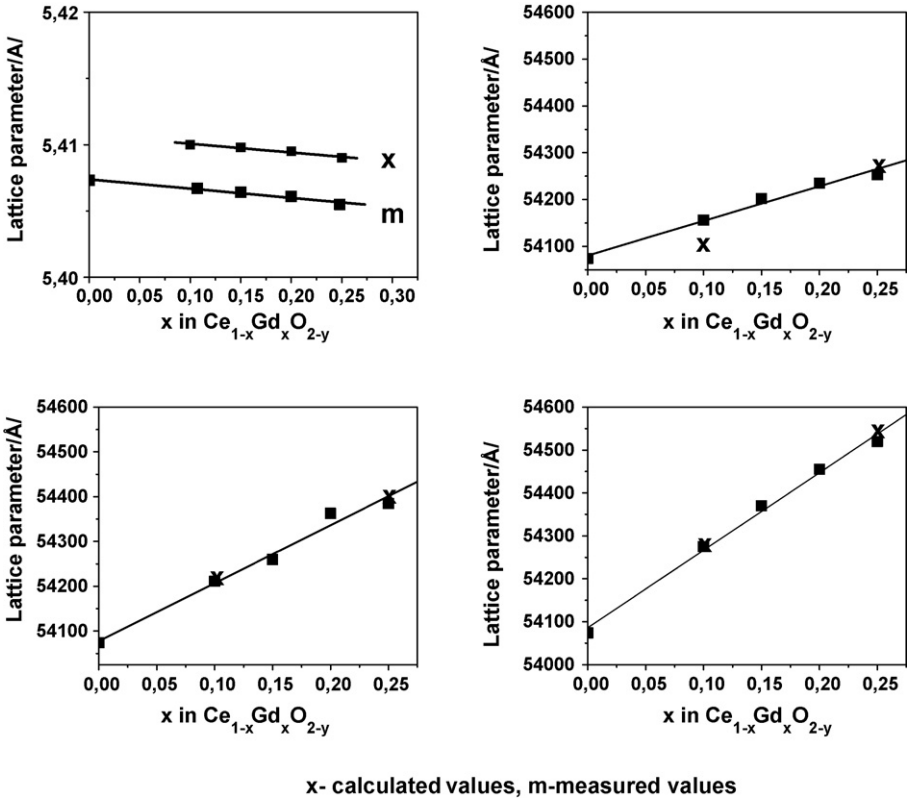

Fig. 4. Lattice parameters of $Ce_{1-x}Re_xO_{2-y}$ vs. dopants concentration (x = 0–0.25).

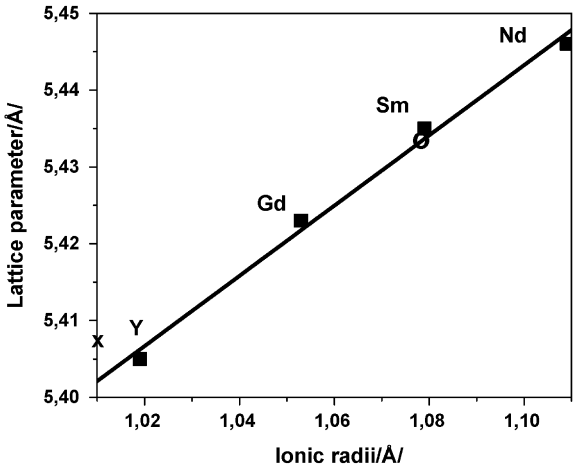

Fig. 5. Lattice parameters of $Ce_{0.8}Re_{0.2}O_{2-y}$ as a function of ionic radii (×—measured lattice parameter of un-doped ceria; ■—measured lattice parameters of solid solutions with $x = 0.2$; ○—average ionic radius of all the dopants present in the lattice).

concentration of dopants ($x = 0.20$) as shown in Fig. 5. From this diagram we obtained the average ionic radius of 1.078 Å (marked as o in Fig. 5) for the measured value of lattice parameter 5.434 Å.

Taking the value of 1.078 Å as r_M as well as the value of x obtained from chemical analysis (0.206 from Table 1) the lattice parameter was calculated according to Eq. (2). The value of 5.436 Å is in very good agreement with the measured lattice parameter of co-doped sample.

According to this model we also calculated theoretical densities of all studied compositions. These results are presented in Table 4.

The slope of each individual line in Fig. 4 was plotted versus ionic radii and the data are given in Fig. 6. The value of 1.020 Å for the critical ionic radius was obtained from this diagram.

Table 4
Theoretical densities of rare earth doped ceria

No. of sample	Composition	Theoretical density (g/cm^3) (calculated from X-ray data)
1	CeO_{2-y}	7.231
2	$Ce_{0.90}Y_{0.10}O_{2-y}$	6.974
3	$Ce_{0.85}Y_{0.15}O_{2-y}$	6.861
4	$Ce_{0.80}Y_{0.20}O_{2-y}$	6.738
5	$Ce_{0.75}Y_{0.25}O_{2-y}$	6.616
6	$Ce_{0.90}Nd_{0.10}O_{2-y}$	7.134
7	$Ce_{0.85}Nd_{0.15}O_{2-y}$	7.089
8	$Ce_{0.80}Nd_{0.20}O_{2-y}$	7.048
9	$Ce_{0.75}Nd_{0.25}O_{2-y}$	7.015
10	$Ce_{0.90}Sm_{0.10}O_{2-y}$	7.185
11	$Ce_{0.85}Sm_{0.15}O_{2-y}$	7.170
12	$Ce_{0.80}Sm_{0.20}O_{2-y}$	7.134
13	$Ce_{0.75}Sm_{0.25}O_{2-y}$	7.130
14	$Ce_{0.90}Gd_{0.10}O_{2-y}$	7.236
15	$Ce_{0.85}Gd_{0.15}O_{2-y}$	7.237
16	$Ce_{0.80}Gd_{0.20}O_{2-y}$	7.242
17	$Ce_{0.75}Gd_{0.25}O_{2-y}$	7.254
18	$Ce_{0.80}Y_{0.05}Nd_{0.05}Sm_{0.05}Gd_{0.05N}O_{2-y}$	7.019

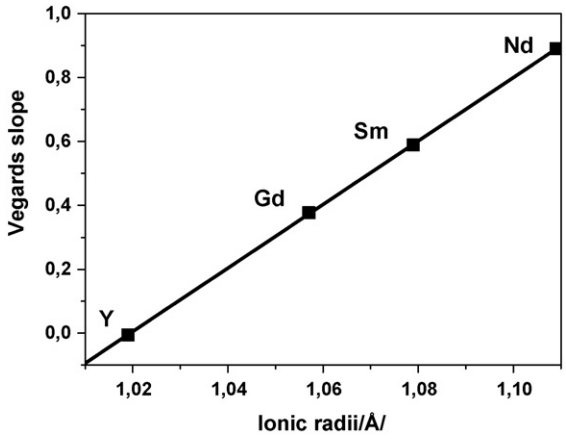

Fig. 6. The slope in Fig. 4 vs. cation radius (Å) from (Ref. [16]).

This value is defined as the ionic radius of the dopant that causes neither expansion nor contraction of the fluorite lattice which is an important parameter in tailoring electrical conductivity of ceria based materials. The critical ionic radius can also be obtained from Fig. 5, using the measured lattice parameters. The value of 1.024 Å is obtained for critical ionic radius taking 5.411 Å for the lattice constant of pure ceria. This value is very similar to the previous value and is nearly the same as obtained by Rey et al. [12].

Our calculations showed that the model that takes into account the existence of anion vacancies in the lattice can be applied to calculate lattice parameter of both single and multiple doped nanometric ceria. The value of the critical ionic radius experimentally obtained and the one calculated by plotting the slopes versus ionic radius agree with the value published in the literature [12].

4. Conclusions

Glycine/nitrate process was modified by substituting part of Ce-nitrate for Ce-acetate, and applied to produce, for the first time, single and multiple doped ceria solid solutions. The advantages of this method are as follows:

- large amount of powder can be produced in a very short time;
- single phase nanopowders with high specific surface area can be obtained;
- no intermediate phases are detected;
- preparation equipment is very simple;
- very precise control of stoichiometry has been demonstrated over all the batches;
- the method is flexible for forming complex compositions.

A model which introduced effective anion vacancies radius was applied to calculate lattice parameter of single and co-doped samples. It was found that by using the average ionic radius of measured lattice parameter dependence versus ionic radii for constant concentration of dopants, the model could be applied to calculate lattice parameter of multiple doped solid solutions.

Acknowledgements

The authors are grateful to A. von Humboldt Foundation, Germany for supporting this work. We also acknowledge the help of MSEP of Serbia for supporting the Project No. 142003.

References

[1] L.A. Chick, G.D. Maupin, L.R. Pederson, Nanostruct. Mater. 4 (1994) 603–615.
[2] T. Tsuzuki, P.G. McCormick, J. Am. Ceram. Soc. 84 (2001) 1453–1458.
[3] L.X. Yin, Y.Q. Wang, G.S. Pang, J. Colloid Interface Sci. 246 (2002) 78–83.
[4] X. Yu, F. Li, X. Ye, X. Xin, Z. Xue, J. Am. Ceram. Soc. 83 (2000) 964–966.
[5] M.M. Amala Sekar, S. Sundar Manoharan, K.C. Patil, J. Mater. Sci. Lett. 9 (1990) 1205–1207.
[6] L.A. Chick, L.R. Robertson, G.D. Maupin, J.L. Bates, L.E. Thomas, G.J. Exarhos, Mater. Lett. 10 (1999) 6–12.
[7] W. Chen, F. Li, J. Yu, Mater. Lett. 60 (2006) 57–62.
[8] S.B. Bošković, B.Z. Matovic, M.D. Vlajić, V.D. Kristić, Ceram. Int. 33 (1) (2007) 89–93.
[9] B. Lönnberg, J. Mater. Sci. 29 (29) (1994) 3224–3230.
[10] J. van Herle, D. Senevirante, A.J. McEvoy, J. Eur. Ceram. Soc. 19 (1999) 837–841.
[11] J.F.Q. Rey, E.N.S. Muccillo, J. Eur. Ceram. Soc. 24 (2004) 1287–1290.
[12] S.J. Hong, A.V. Virkar, J. Am. Ceram. Soc. 78 (1995) 433–439.
[13] F. Zhang, S.-W. Chang, J.E. Spanier, E. Apak, Q. Jin, Appl. Phys. Lett. 80 (2002) 127–129.
[14] Z.D. Dohcevic-Mitrovic, M. Grujic-Brojcin, M. Scepanovic, Z.V. Popovic, S. Boskovic, B. Matovic, M. Zinkevich, F. Aldinger, J. Phys. Condens. Matter 18 (2006) 1–8.
[15] Z.D. Dohcevic-Mitrovic, M. Grujic-Brojcin, M. Scepanovic, Z.V. Popovic, S. Boskovic, B. Matovic, M. Zinkevich, F. Aldinger, Solid State Commun. 137 (2006) 387–390.
[16] R.D. Shannon, Acta Crystallogr. A32 (1976) 751–767.
[17] H. Deguchi, H. Yoshida, T. Inagaki, M. Hirouchi, Solid State Ionics 176 (2005) 1817–1825.